Supplemental Online Content

Magliyah MS, Geuer S, Alsalamah AK, Lenzner S, Drasdo M, Schatz P. Association of the recurrent rare variant c.415T>C p.Phe139Leu in *CLN5* with a recessively inherited macular dystrophy. *JAMA Ophthalmol*. Published online January 28, 2021. doi:10.1001/jamaophthalmol.2020.6085

eFigure 11. Multimodal retinal imaging in Patient 7 with a nonsyndromic macular dystrophy and the homozygous c.415T>C (p.Phe139Leu) missense variant in CLN5

eFigure 12. Electroretinogram of Patient 7 with the homozygous c.415T>C (p.Phe139Leu) missense variant in CLN5

eResults

eReferences

This supplemental material has been provided by the authors to give readers additional information about their work.

eMethods

Genetic testing

Genetic testing including next generation sequencing and whole exome sequencing (NGS and WES). For NGS analysis, genomic DNA (buccal swab and/or EDTA blood) of the patients was fragmented using a Covaris E220 evolution (Covaris, Woburn MA, U.S.A.). Libraries were prepared using NEB Ultra II kits (New England Biolabs, Ipswich MA, U.S.A.) and enriched by a customized panel for retinal dystrophies or by Roche SeqCap EZ MedExome V1 target enrichment for exome sequencing (both from Roche, Madison WI, U.S.A.). Sequencing was performed on an Illumina system (NovaSeq 6000, NextSeq 500, HiSeq 1500 or MiSeq (Illumina, San Diego CA, U.S.A.). NGS data were aligned to the hg19 genome assembly. Variant calling and annotation was performed by an inhouse developed bioinformatics pipeline (Bioscientia, Ingelheim, Germany). Identified SNVs and indels were filtered against external and internal databases focusing on rare variants with a minor allele frequency (MAF) in gnomAD of 1% or less and removing known artefacts and variants in regions with highly homologous regions. Classification of variants was conducted based on ACMG guidelines (Richards et al., 2015)[1] considering database entries (incl. HGMD, Qiagen, Hilden, Germany), bioinformatics prediction tools and literature status.

For Sanger sequencing genomic DNA of the respective family members was screened for the *CLN5* c.415T>C variant. For this, the corresponding exon was amplified by polymerase chain reaction (PCR) (forward primer: cagcatggaagaacagctgaac, reverse primer: ccaaaagtacattttacaaatgacctc) and analyzed by direct sequencing on an AB 3500 xL sequencer (Applied Biosystems, Foster City CA, U.S.A.). The resulting sequence data

were compared to the reference sequence NM_006493.4 (SeqPilot, JSI medical systems, Ettenheim Germany). Reported variants were assessed using gnomAD (https://gnomad.broadinstitute.org/, v3, access date 13/12/2019).

Genes covered by the latest version of the customized NGS-panel for retinal dystrophies: *ABCA4, ABHD12, ACACB, ACBD5, ACO2, ADAM9, ADAMTS18, ADGRA3, ADGRV1, ADIPOR1, AFG3L2, AGBL5, AHI1, AIPL1, ALMS1, ANTXR1, ARL13A, ARL2BP, ARL6, ARSG, ASAP1, ASRGL1, ATF6, ATP13A2, ATP1A3, BBIP1, BBS1, BBS10, BBS12, BBS2, BBS4, BBS5, BBS7, BBS9, BCOR, BEST1, C12orf65, C1QTNF5, C8orf37, CA4, CABP4, CACNA1F, CACNA2D4, CAPN5, CBY1, CC2D2A, CCDC28B, CCT2, CDH16, CDH23, CDH3, CDHR1, CEP131, CEP164, CEP19, CEP250, CEP290, CEP72, CERKL, CFAP410, CFH, CHM, CIB2, CISD2, CLN3, CLN5, CLN6, CLN8, CLRN1, CNGA1, CNGA3, CNGB1, CNGB3, CNNM4, COL9A1, CORO2B, CRB1, CRX, CSTB, CTNNA1, CTSD, CTSF, CYP4V2, DHDDS, DHX38, DNAJC17, DNAJC5, DRAM2, DTHD1, ELOVL4, EMC1, ERCC6, EVC, EVC2, EYS, FA2H, FAM161A, FBLN5, FBN3, FLVCR1, FSCN2, FSTL1, GDF6, GNAT1, GNAT2, GNB3, GNPTG, GNS, GPR179, GRID2, GRK1, GRM6, GRN, GUCA1A, GUCA1B, GUCY2D, HARS1, HARS2, HGSNAT, HK1, HMCN1, IDH3B, IFT140, IFT172, IFT27, IFT74, IKBKG, IMPDH1, IMPG1, IMPG2, INVS, IQCB1, ITM2B, KCNJ13, KCNV2, KCTD7, KIAA1549, KIF11, KIF5A, KIZ, KLHL7, LAMA1, LCA5, LRAT, LRIT3, LZTFL1, MAK, MERTK, MFN2, MFSD8, MIR204, MKKS, MKS1, MPDZ, MT-ATP6, MT-ND1, MT-ND4, MT-ND6, MT-TH, MT-TL1, MT-TP, MT-TS2, MTTP, MVK, MYO7A, NBAS, NDRG4, NEK2, NEUROD1, NMNAT1, NPHP3, NR2E3, NR2F1, NRL, NYX, OAT, OFD1, OPA1, OPA3,*

OR2W3, OTX2, PANK2, PCARE, PCDH15, PCYT1A, PDE6A, PDE6B, PDE6C, PDE6G, PDE6H, PDZD7, PEX1, PEX10, PEX11B, PEX12, PEX13, PEX14, PEX16, PEX19, PEX2, PEX26, PEX3, PEX5, PEX6, PEX7, PGK1, PHYH, PITPNM3, PLA2G5, PLK4, PNPLA6, POC1A, POC1B, POC5, PPT1, PRCD, PRDM13, PRICKLE2, PROM1, PRPF3, PRPF31, PRPF4, PRPF6, PRPF8, PRPH2, PRPS1, RAB28, RAX2, RB1, RBP3, RBP4, RCBTB1, RD3, RDH11, RDH12, RDH5, RGR, RGS9, RGS9BP, RHBDD2, RHO, RIMS1, RLBP1, ROM1, RP1, RP1L1, RP2, RP9, RPE65, RPGR, RPGRIP1, RPGRIP1L, RTN4IP1, SAG, SCAPER, SDCCAG8, SEMA4A, SLC24A1, SLC25A46, SLC7A14, SNRNP200, SPATA7, SPG7, SPP2, TEAD1, TIMM8A, TIMP3, TMEM126A, TMEM216, TMEM237, TOPORS, TPP1, TRAF3IP1, TRAPPC3, TRIM32, TRNT1, TRPM1, TTC8, TTLL5, TTPA, TUB, TUBGCP4, TUBGCP6, TULP1, UCHL1, UNC119, USH1C, USH1G, USH2A, VAX2, WASF3, WDPCP, WDR19, WFS1, WHRN, XPNPEP2, XPNPEP3, YME1L1, ZNF408, ZNF423, ZNF51.

Functional prediction tools:

SIFT ensembl 66, SIFT4G 2.4, PROVEAN 1.1 ensembl 66, Polyphen-2 v2.2.2, LRT, MutationTaster 2, MutationAssessor release 3, FATHMM v2.3, fathmm-MKL, fathmm-XF, CADD v1.4, VEST v4.0, fitCons v1.01, LINSIGHT, DANN, MetaSVM, MetaLR, GenoCanyon v1.0.3, Eigen & Eigen PC v1.1, M-CAP v1.3, REVEL, MutPred v1.2, MVP 1.0, MPCrelease1, PrimateAI, deogen2, ALoFT 1.0

Conservation tools:

phyloP100way_vertebrate (hg38), phyloP30way_mammalian (hg38), phyloP17way_primate (hg38), phastCons100way_vertebrate (hg38)

phastCons30way_mammalian (hg38), phastCons17way_primate (hg38), GERP++, SiPhy, bStatistic.

Ophthalmological and neurological examination

Multimodal retinal imaging included transfoveal horizontal spectral domain optical coherence tomography scans (SD-OCT, Spectralis OCT, Heidelberg Engineering, Inc., Heidelberg, Germany). Retinal thickness in patients was compared to that of controls from a previously published paper by us.[2] Wide field imaging including fundus autofluorescence (Optos PLC, Dunfermline, UK) was performed in all patients except patient 3, who had imaging with a fundus camera (Topcon TRC-50DX, Topcon Medical Systems, Inc., NJ, US).

Electrophysiological testing was carried out according to ISCEV standards,[3] with a few modifications as described by us previously.[2,4]

Parapapillary nerve fiber layer thickness was evaluated with Copernicus SD-OCT (Optopol Technology, Zawiercie, Poland). Color vision was estimated with Ishihara plates. Visual fields were measured using Humphrey 30-2 perimetry.

Magnetic resonance imaging (MRI) of the brain and optic nerves was done with a 3-Tesla MRI.

eReferences

1. Richards S, Aziz N, Bale S, Bick D, Das S, Gastier-Foster J, Grody WW, Hegde M, Lyon E, Spector E, Voelkerding K, Rehm HL; ACMG Laboratory Quality Assurance Committee. Standards and guidelines for the interpretation of sequence variants: a joint consensus recommendation of the American College of Medical Genetics and Genomics and the Association for Molecular Pathology. Genet Med. 2015;17(5):405-424.

2. Al-Hujaili H, Taskintuna I, Neuhaus C, et al. Long-term follow-up of retinal function and structure in TRPM1-associated complete congenital stationary night blindness. *Mol Vis*. 2019;25:851-858.

3. McCulloch DL, Marmor MF, Brigell MG, et al. ISCEV Standard for full-field clinical electroretinography (2015 update). *Doc Ophthalmol*.2015;130:1–12.

4. Magliyah MS, AlSulaiman SM, Schatz P, Nowilaty SR. Evolution of macular hole in enhanced S-cone syndrome. *Doc Ophthalmol*. https://doi.org /10.1007/s10633-020-09787-8. 2020.08.19.

eTable 1. Clinical findings in a cohort of patients with a nonsyndromic macular dystrophy. All patient had the homozygous *CLN5* missense variant c.415T>C (p.Phe139Leu).

Patient	Age in decades	Years of follow-up	VA OD:OS at 1st visit, VA OD:OS at most recent visit	Refraction 1st visit OD (SE), OS (SE)	Type of genetic testing	*CLN5* gene sequence variant	Follow up duration (years)
1	4	2	20/125: 20/100, 20/100: 20/100	-	NGS	c.415T>C (p.Phe139Leu)	2
2	6	4	20/160: 20/100, 20/200: 20/200	-2.25 -2.75 x150 (-3.62), -1.50 -3.25 x155 (-3.13)	NGS	c.415T>C (p.Phe139Leu)	4
3	6	1	20/400: 20/200	-	NGS	c.415T>C (p.Phe139Leu)	1
4	4	1	20/60: 2/200, 20/100: 20/160	-1.00 -0.50 x80 (-1.25), -1.25	NGS WES	c.415T>C (p.Phe139Leu)	1
5	4	5	20/300: 20/300, 20/100: 20/100	-2.00 -0.50 x135 (-2.25), -2.00 -1.00 x90 (-2.50)	NGS WES	c.415T>C (p.Phe139Leu)	5
6	4	4	20/80: 20/60, 20/100: 20/100	-1.50, -1.00	NGS	c.415T>C (p.Phe139Leu). And two heterozygous missense variants c.11008G>A p. (Glu3670Lys) and c.15281C>T p. (Pro5094Leu) in *USH2A* with unclear pathogenic significance†	4
7	6	1	4/200: 20/300, 1/200: 1/200	-	NGS	c.415T>C (p.Phe139Leu)	1

VA=best corrected visual acuity. M= male. F= female. OD=right eye. OS=left eye. SE=spherical equivalent. NGS= next-generation sequencing. WES= whole-exome sequencing. † The missense variants Glu3670Lys and Pro5094Leu have frequencies of 1.31e-4 and 5.3e-5, respectively, in gnomad (https://gnomad.broadinstitute.org/, access date 2020 October 6). None of these variants is completely conserved among the species listed in https://genome.ucsc.edu/, access date 2020 October 6). In addition, Glu3670Lys is classified as likely benign and Pro5094Leu as being of uncertain significance in ClinVar https://www.ncbi.nlm.nih.gov/clinvar/, access date 2020 October 6.

eTable 2. Full-field electroretinogram (ERG) and optical coherence tomography (OCT) findings in 7 patients with a nonsyndromic macular dystrophy and the homozygous c.415T>C (p.Phe139Leu) missense variant in *CLN5*. CMT= central macular thickness. A=amplitude in microvolts. It=implicit time in milliseconds. OD=right eye. µm=micrometers. * Reference material for optical coherence tomography (OCT) from Al-Hujaili et al.[1] ERG and OCT central subfield thickness (CST) values shown are for OD for all patients. †ERGs are given as: ERG at first visit, ERG at follow-up (if any). FU=Follow-up.

Patient	OCT CST OD 1st visit, FU (µm)	Macular volume OD 1st visit, FU (mm^3)	ERG† Rod		ERG Rod- cone a Wave		ERG Rod- cone b Wave		ERG Cone a Wave		ERG Cone b Wave		ERG 30 Hz Flicker	
			A	It	A	It	A	It	A	It	A	It	A	It
1	105, 104	-	206	106	264	22	436	50	116	15	211	36	129	28
2	115, 114	5.40, 5.48	217	64	198	20	286	59	29	13	60	35	92	34
3	-	-	-	-	-	-	-	-	-	-	-	-	-	-
4	87, 69	6.29	480	64	262	20	475	66	54	18	85	37	112	34
5	89, 51	4.52	246, 372	104, 67	375, 366	15, 18	598, 541	48, 64	132, 60	15, 16	195, 112	37, 36	210, 166	29, 34
6	51	-	167	85	179	21	491	41	84	14	226	32	141	26
7	62	4.18	261	63	186	19	337	56	33	16	96	39	94	36

Normal	246-283	8.27-9.15	103-380	69-115	164-378	11-17	284-705	42-60	54-117	11-15	96-239	33-37	96-259	25-32

eReference

1. Al-Hujaili H, Taskintuna I, Neuhaus C, et al. Long-term follow-up of retinal function and structure in TRPM1-associated complete congenital stationary night blindness. *Mol Vis*. 2019;25:851-858.

eFigure 1. Multimodal retinal imaging in Patient 1 with a nonsyndromic macular dystrophy and the homozygous c.415T>C (p.Phe139Leu) missense variant in *CLN5*. Top panel: Fundus imaging shows macular degeneration and temporally pale and excavated discs. Middle panel: Fundus autofluorescence shows a characteristic central macular hypoautofluorescence.

Lower panel: Transfoveal horizontal spectral domain optical coherence tomography scans showing a central loss of photoreceptors, corresponding to the area of loss of autofluorescence.

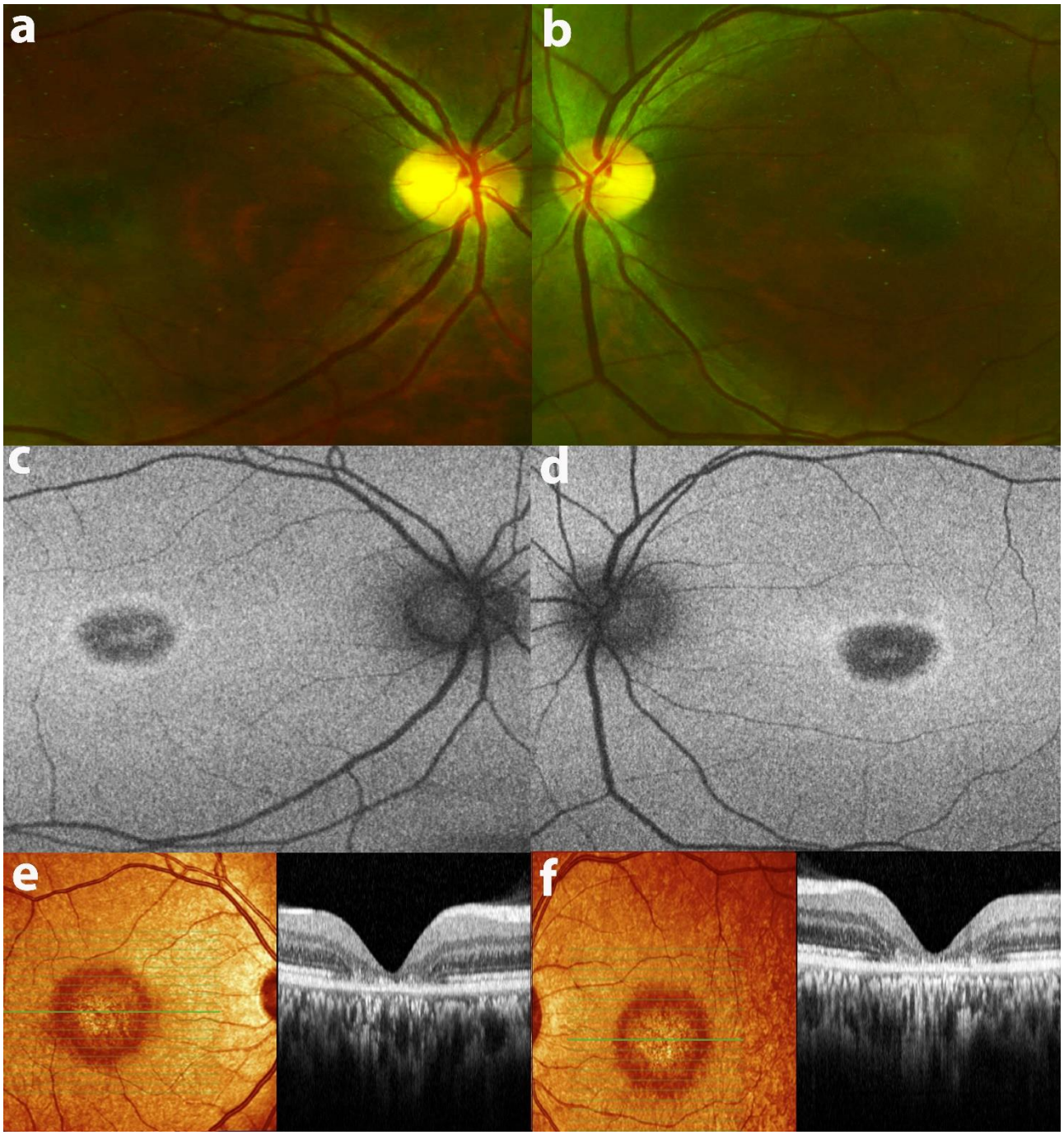

eFigure 2. Electroretinogram of Patient 1. Ms=milliseconds. µV=microvolts

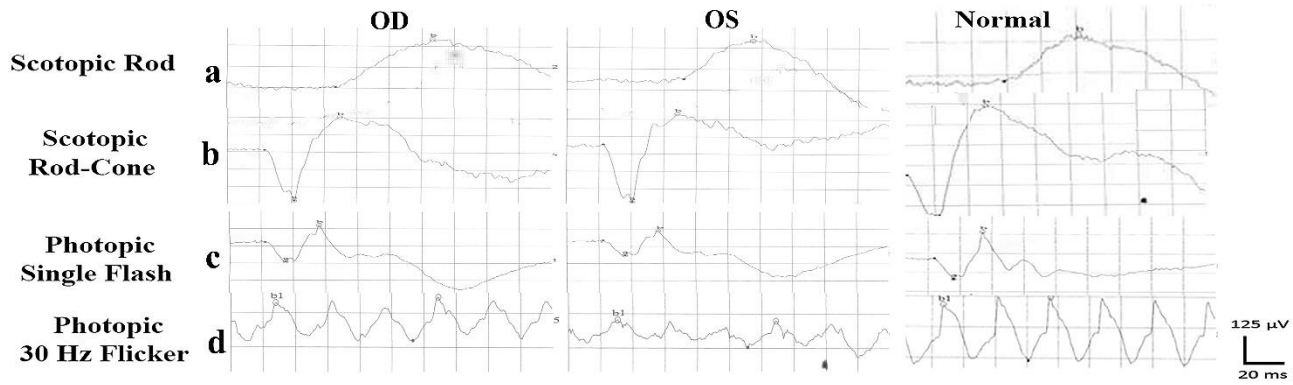

eFigure 3. Multimodal retinal imaging in Patient 2 with a nonsyndromic macular dystrophy and the homozygous c.415T>C (p.Phe139Leu) missense variant in *CLN5*. Top panel: Fundus imaging shows macular degeneration and temporally pale and excavated discs. Middle panel: Fundus autofluorescence shows a characteristic central macular hypoautofluorescence.

Lower panel: Transfoveal horizontal spectral domain optical coherence tomography scans showing a central loss of photoreceptors, corresponding to the area of loss of autofluorescence.

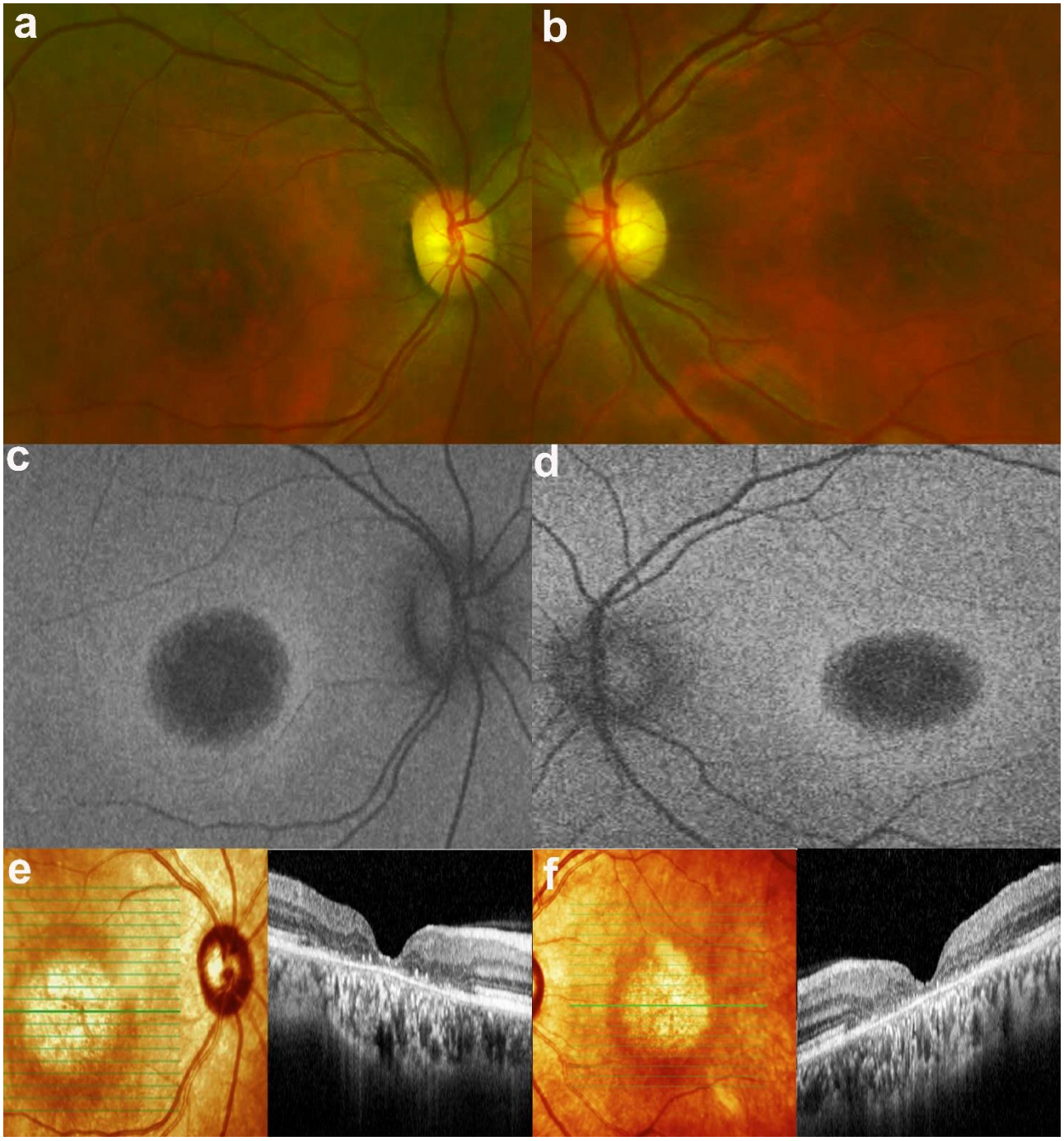

eFigure 4. Electroretinogram of Patient 2 with the homozygous c.415T>C (p.Phe139Leu) missense variant in *CLN5*. Ms=milliseconds. µV=microvolts

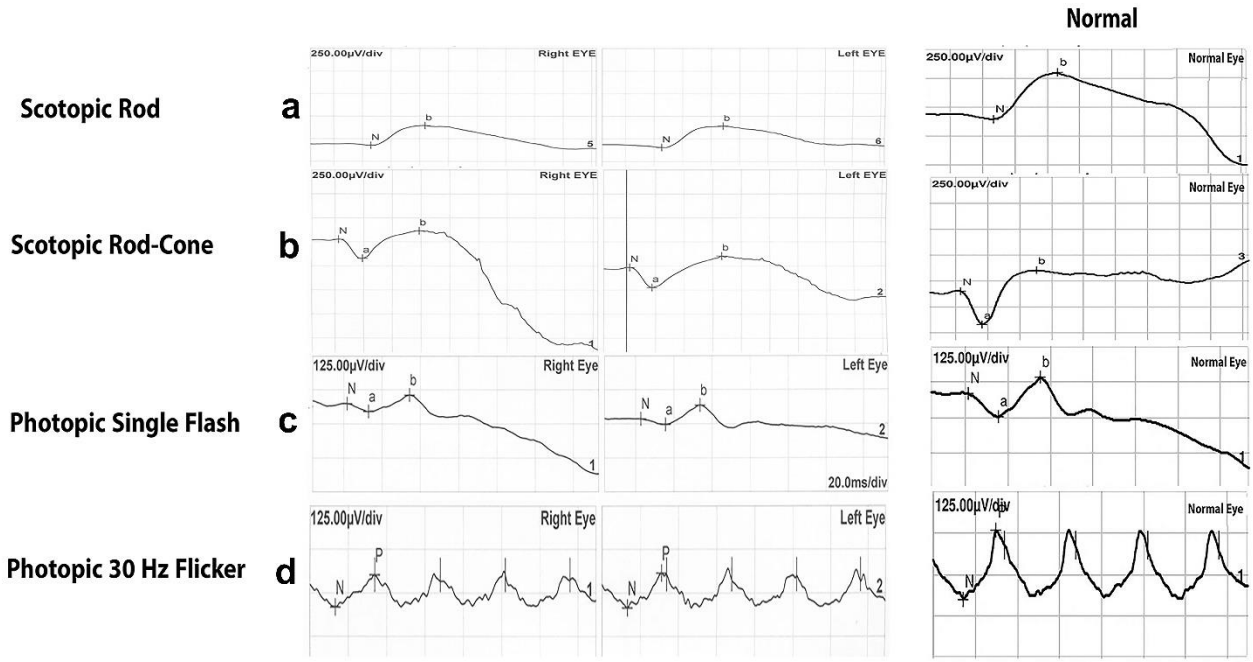

eFigure 5. Color fundus image in the right eye of Patient 3 with a nonsyndromic macular dystrophy and the homozygous c.415T>C (p.Phe139Leu) missense variant in *CLN5*.

eFigure 6. Electroretinogram of Patient 4 with the homozygous c.415T>C (p.Phe139Leu) missense variant in *CLN5*. Ms=milliseconds. µV=microvolts.

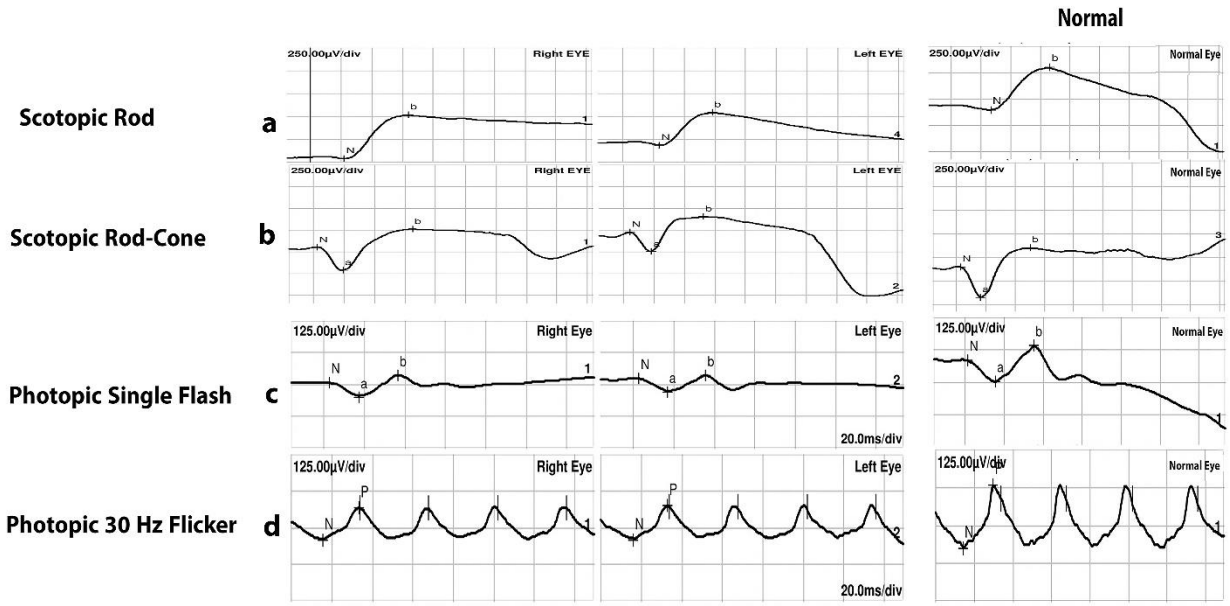

eFigure 7. Multimodal retinal imaging in Patient 5 with a nonsyndromic macular dystrophy and the homozygous c.415T>C (p.Phe139Leu) missense variant in *CLN5*. Top panel: Fundus imaging shows macular degeneration and temporally pale and excavated discs.

Middle panel: Fundus autofluorescence shows a characteristic central macular hypoautofluorescence.

Lower panel: Transfoveal horizontal spectral domain optical coherence tomography scans showing a central loss of photoreceptors, corresponding to the area of loss of autofluorescence.

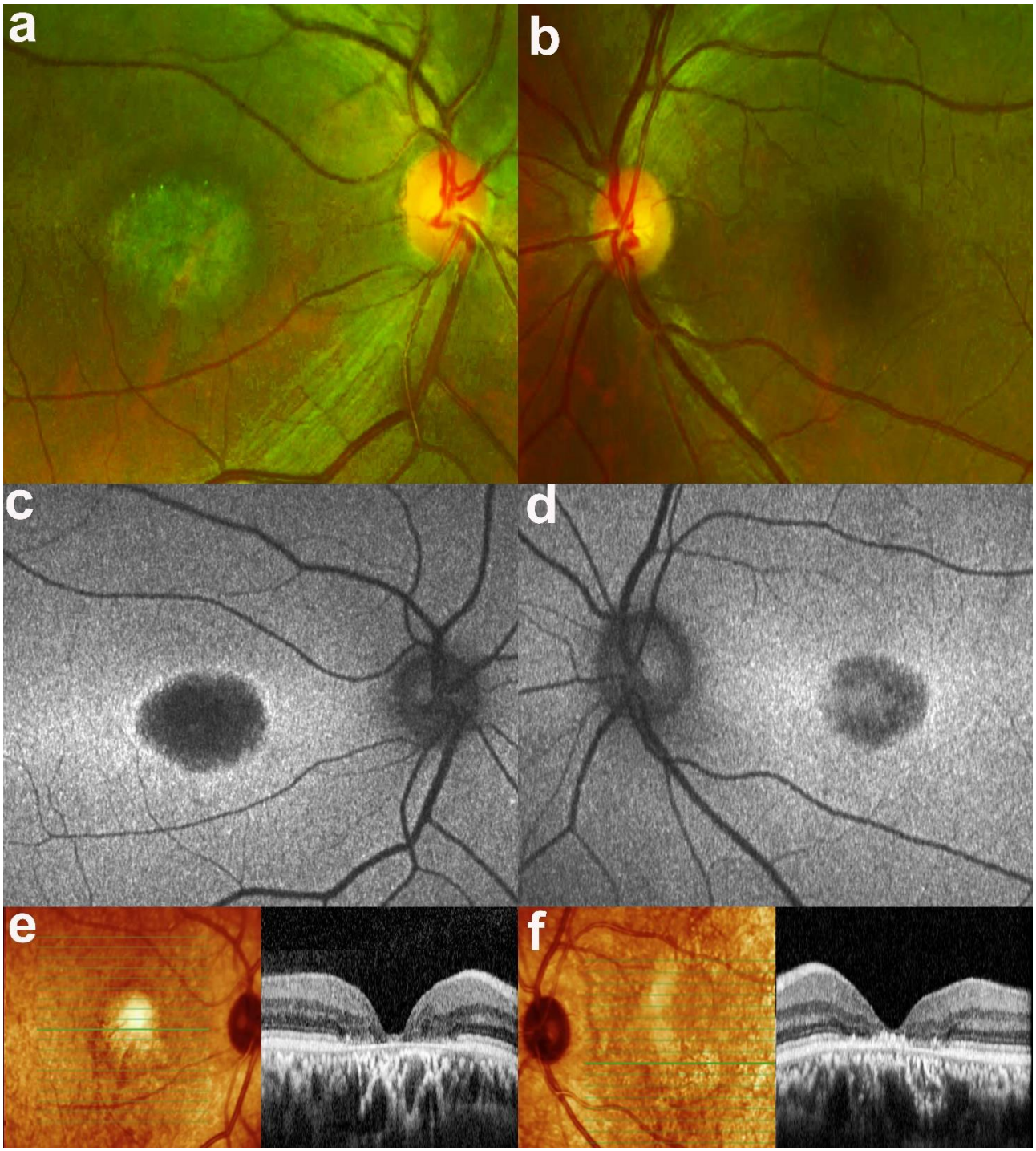

eFigure 8. Electroretinogram of Patient 5 with the homozygous c.415T>C (p.Phe139Leu) missense variant in *CLN5*. Ms=milliseconds. µV=microvolts.

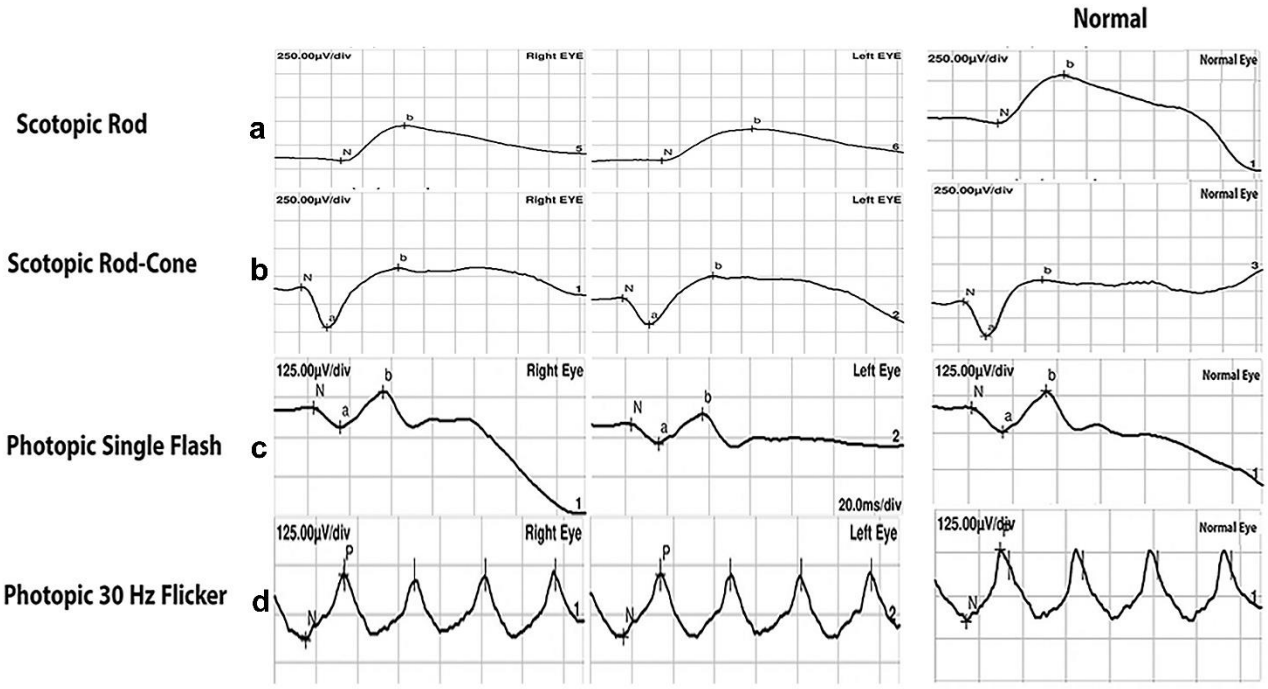

eFigure 9. Multimodal retinal imaging in Patient 6 with a nonsyndromic macular dystrophy and the homozygous c.415T>C (p.Phe139Leu) missense variant in *CLN5*. Top panel: Fundus imaging shows macular degeneration and temporally pale and excavated discs. Middle panel: Fundus autofluorescence shows a characteristic central macular hypoautofluorescence.

Lower panel: Transfoveal horizontal spectral domain optical coherence tomography scans showing a central loss of photoreceptors, corresponding to the area of loss of autofluorescence.

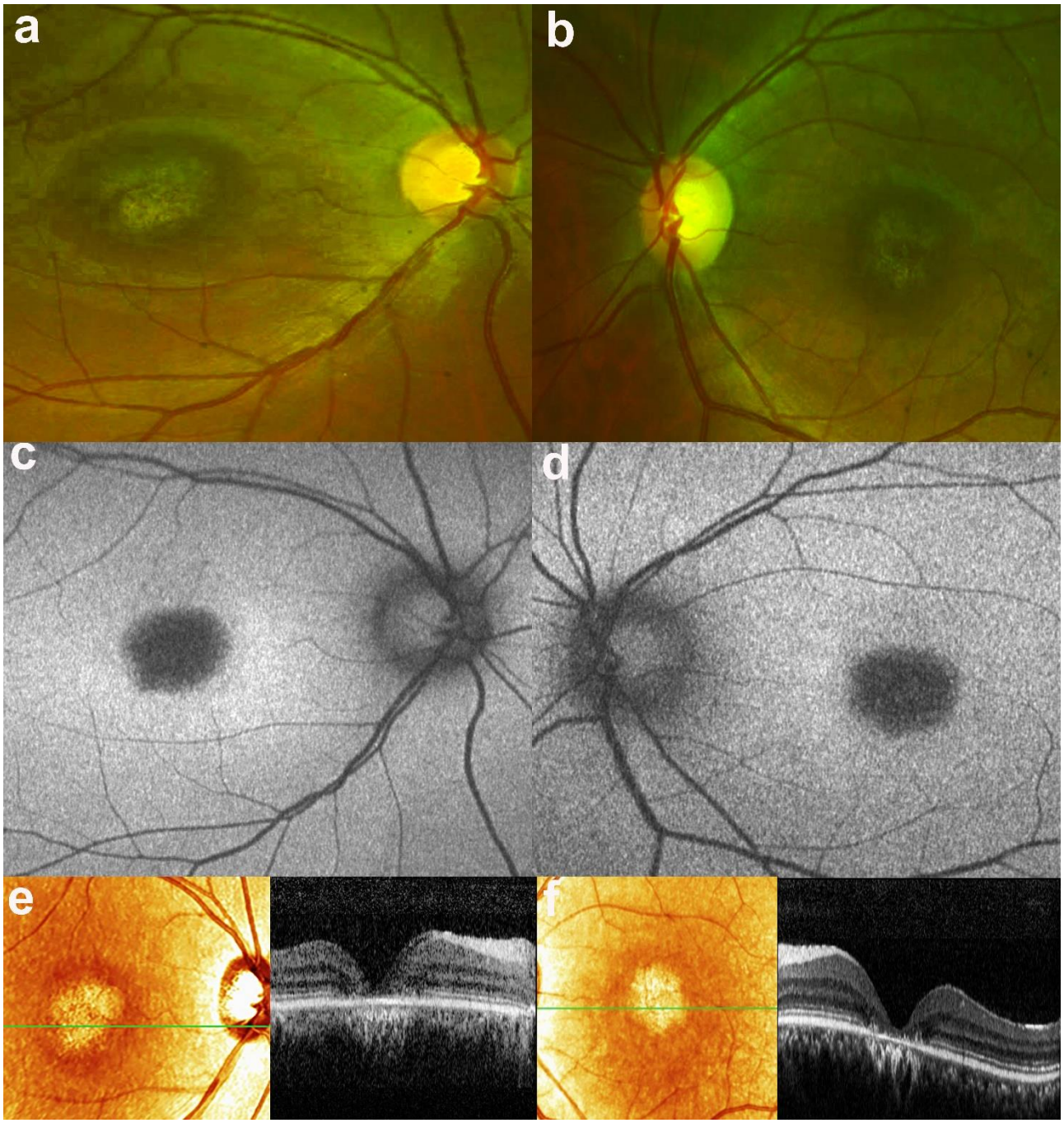

eFigure 10. Electroretinogram of Patient 6 with the homozygous c.415T>C (p.Phe139Leu) missense variant in *CLN5*. Ms=milliseconds. µV=microvolts.

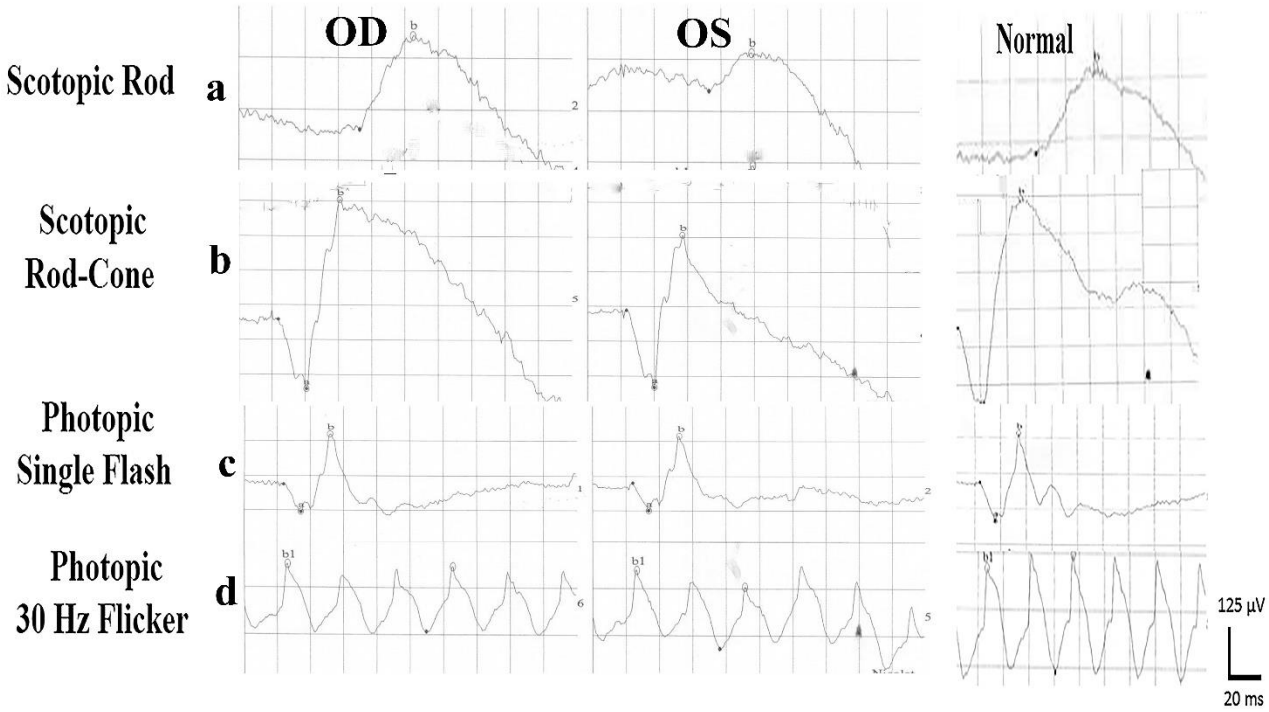

eFigure 11. Multimodal retinal imaging in Patient 7 with a nonsyndromic macular dystrophy and the homozygous c.415T>C (p.Phe139Leu) missense variant in *CLN5*. Top panel: Fundus imaging shows macular degeneration and temporally pale and excavated discs. Middle panel: Fundus autofluorescence shows a characteristic central macular hypoautofluorescence.

Lower panel: Transfoveal horizontal spectral domain optical coherence tomography scans showing a central loss of photoreceptors, corresponding to the area of loss of autofluorescence.

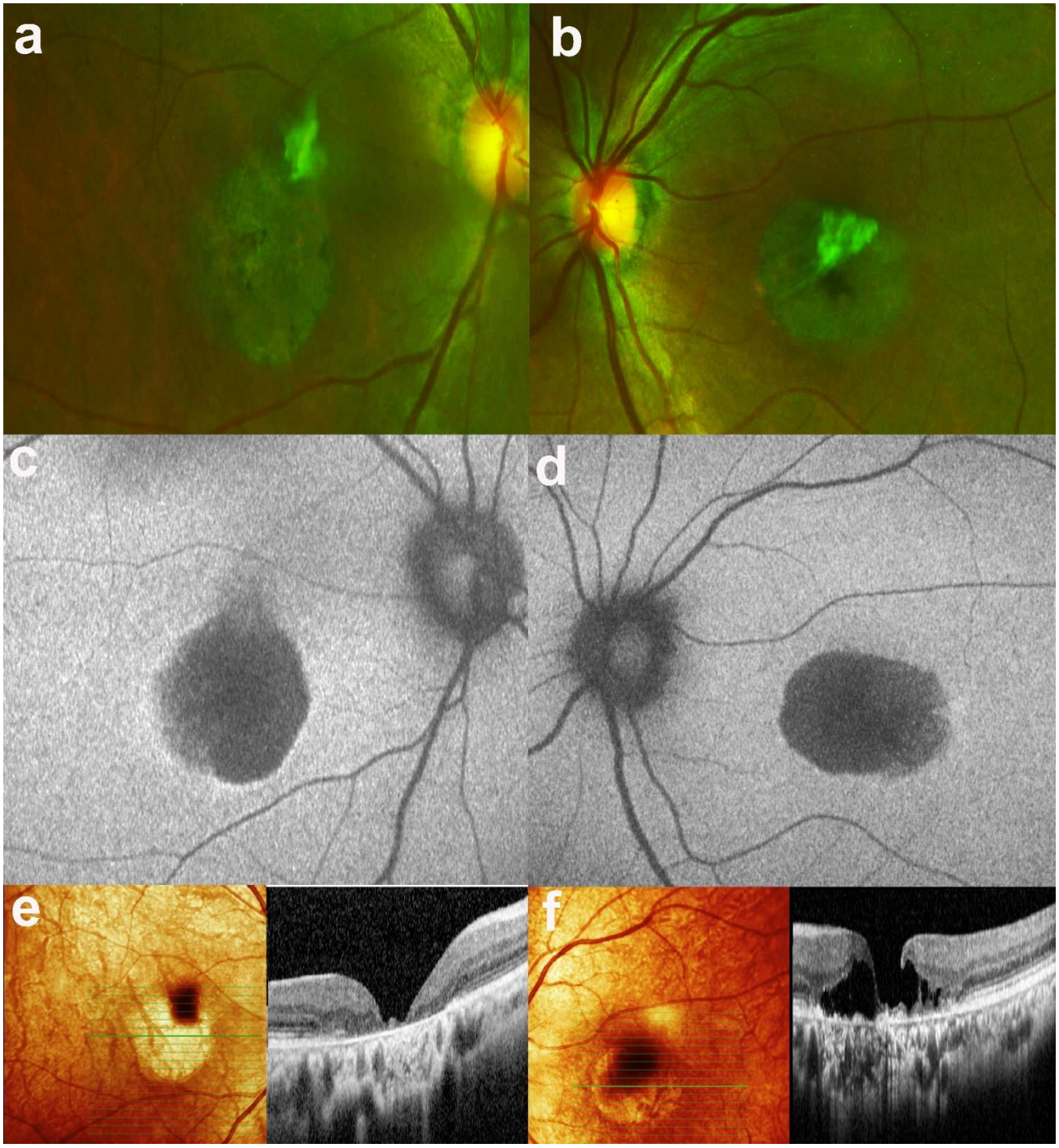

eFigure 12. Electroretinogram of Patient 7 with the homozygous c.415T>C (p.Phe139Leu) missense variant in *CLN5*. Ms=milliseconds. μV=microvolts.

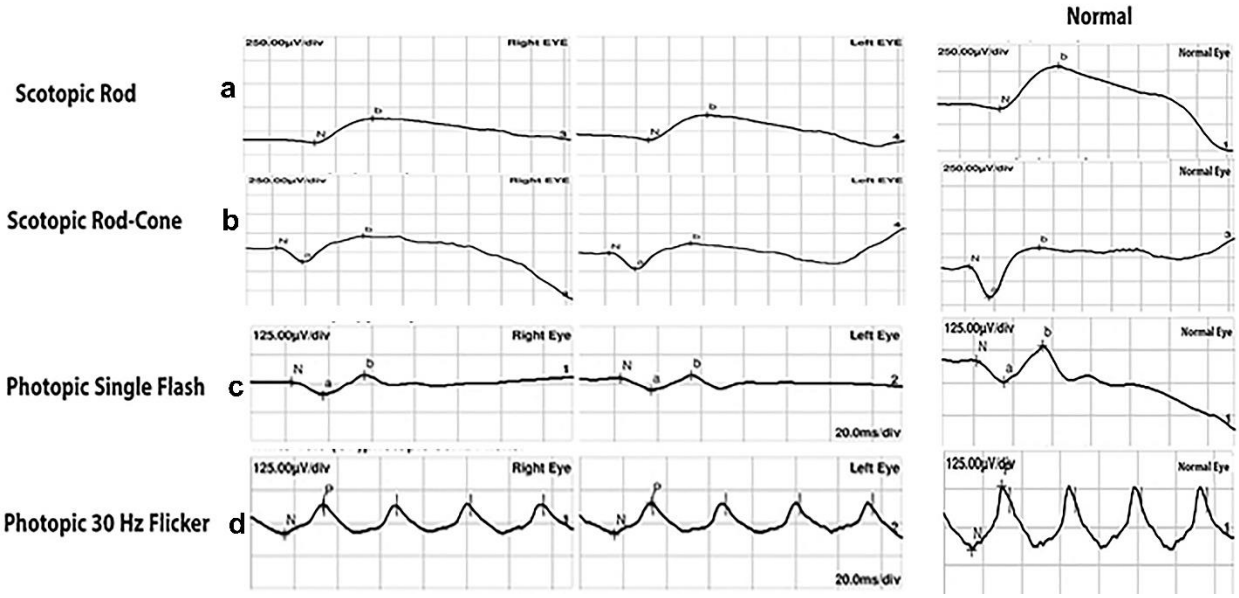

eResults. Additional results of ophthalmological and neurological investigations.

Five of the seven patients had consanguineous parents. All had a negative family history for neurological or retinal disease, except for one of the patients whose uncle suffered from poor vision. Past medical history in this cohort included asthma, hypertension and a single episode of a mild hypertension-related stroke (1 patient, age in decades: 6), acne and depression (1 patient), hypothyroidism (1 patient). The remaining patients did not report any significant past medical history. Occupations included (1 patient for each): military work, business, not working, retired, pharmaceut, office work, retired teacher. Three of the patients were not driving, or had stopped driving, partly because of poor vision. Patients 1 and 2 were fluent in English, in addition to Arabic.

Upon specific questioning regarding any neurological symptoms, 1 of the patients (as described above) had a history of hypertension related stroke, as described above, resulting in dizziness. Magnetic resonance imaging with diffusion tensor imaging (DTI) of the optic nerves and brain in this patient revealed normal brain white matter, no evidence of volume loss, and mild degree of atrophy and abnormal cerebellar folia; changes possibly related to the previous stroke.

Similarly, another 3 patients reported having suffered from dizziness. Of these, MRI had been done by another center about 1 year ago in one of the patients, showing (according to report): "… few bilateral scattered hyperintense subcortical white-matter T2 foci, with no surrounding edema or mass effect, ranging between 2-7 mm, highly suggestive of microvascular white-matter disease", but no other abnormalities. Thus, the MRIs of these 2 patients contrast with the description of marked cerebellar and cortical atrophy in *CLN5*

disease.[1] The remaining two patients who had suffered from dizziness, reported unremarkable findings on MRI or CT scan, done a few years ago in another center, but no written reports were provided to us. One additional patient reported numbness in the neck, but the patient had not been investigated further for this symptom.

The remaining 2 patients denied any neurological symptoms. Thus, neurological symptoms in this cohort were relatively mild (in 5 patients) in the context of *CLN5* disease, or non-existent (in 2 patients). These neurological symptoms may, or may not, be related to the homozygous *CLN5* variant in these patients. Furthermore, all seven patients were fully communicative with normal speech and cognition. None of the patients had any dysarthria or ataxia.

Three patients (Patients 1, 2 and 4) had additional examinations, after the detection of the homozygous missense variant in *CLN5*. A clear dysmetria on finger nose test, with the eyes shut, was demonstrated in the patient with a possible past hypertension-related stroke. However other tests of neurological dysfunction were negative in this patient. Specifically, no dysdiadochokinesia was observed and Rombergs test was within normal limits. The remaining 2 patients (Patients 1 and 4) had unremarkable neurological examination including normal finger-nose test, Romberg and gait. None of the patients showed any tremor.

None of the patients reported any color blindness when specifically questioned. Color vision assessed with Ishihara plates in Patients 1 and 2 showed mild abnormalities, ranging between 7-14 out of 15, in each of the eyes of the 2 patients.

Pattern visual evoked potentials (pVEP) in Patient 1 and 4 revealed severely delayed-P100 Implicit time (msec) OD 227, OS 229 and OD 128, OS 138 (normal mean 92, range

83-101), in Patients 1 and 4, respectively. This is suggestive of optic nerve dysfunction, however Bass et al showed that macular disease can lead to significant delays in the pVEP, in the absence of any optic nerve disease.[2] Patient 2 could not do pVEP because of low visual acuity.

Visual fields in Patients 1 and 2 revealed bilateral central scotomas but preserved peripheral field. Mean deviation (MD) in the right and left eyes was -1.04 decibel (dB) and -2.23, respectively, in Patient 1, and -6.90 and -3.16 in Patient 2. Patient 4 had low visual acuity and severely depressed central and peripheral fields, but there was a low test reliability.

OCT demonstrated a peripapillary nerve fiber layer thickness within normal limits (as provided by the manufacturer) in Patients 1, 2 and 4.

Taken together, these results strongly support that the homozygous variant c.415T>C (p.Phe139Leu) in *CLN5* does not cause any major neurological disease, at least until the age of the most recent examinations of these patients, although some degree of optic nerve dysfunction cannot be ruled out.

eReferences

1. Mancini C, Nassani S, Guo Y, et al. Adult-onset autosomal recessive ataxia associated with neuronal ceroid lipofuscinosis type 5 gene (CLN5) mutations. *J Neurol*. 2015;262(1):173-178.

2. Bass SJ, Sherman J, Bodis-Wollner I, Nath S. Visual evoked potentials in macular disease. *Invest Ophthalmol Vis Sci.* 1985;26(8):1071-1074.